J. Fluid Mech. (1982), *vol.* 118, *pp.* 205–219
Printed in Great Britain

Comparison of direct numerical simulations with predictions of two-point closures for isotropic turbulence convecting a passive scalar

By JACKSON R. HERRING AND ROBERT M. KERR†
National Center for Atmospheric Research, Boulder, Colorado 80307, U.S.A.

(Received 22 June 1981 and in revised form 8 October 1981)

Results of direct numerical simulations (DNS) for the decay of an initially Gaussian field of turbulence convecting a passive scalar are compared with equivalent results for the direct-interaction approximation (DIA) and the test-field model (TFM). The Taylor microscale Reynolds number R_λ and the equivalent Péclet number P_λ of the comparison ranged from 20–8 and 10–4, respectively. The Prandtl number Pr equals 0·5. Our results show a satisfactory agreement of both theories and numerical simulations, with the DIA giving better overall agreement, especially at small scales. This improved small-scale agreement – which appears to hold up to $R_\lambda \simeq 30$ – is related to the relatively long coherence times of the small scales, and to the fact that the TFM, containing as it does a built-in compliance to the fluctuation dissipation theorem, cannot properly cope with this fact. We also give a comparison of results for the velocity skewness with the experiments of Tavoularis, Bennett & Corrsin (1978).

1. Introduction

Two-point closures such as the test-field model (TFM) (Kraichnan 1971; Newman & Herring 1979) and the related eddy-damped quasinormal approximation (Orszag 1974; Lesieur & Schertzer 1978) appear to explain many of the qualitative characteristics of the experimental data for spectra, decay rates and skewnesses (Larcheveque *et al.* 1980), although detailed comparisons with experiment are only moderately successful. (See the comparison of TFM with the wind-tunnel data of Yeh & Van Atta (1973), reported by Newman & Herring (1979).) This apparent overall success seems in conflict with certain experimental observations; strong intermittency is known to contradict the near-Gaussianity of the multivariate distribution function needed to justify such moment closures (Kraichnan 1968; Frisch & Morff 1981).

The comparison of direct numerical simulations (DNS) with the direct-interaction approximation (DIA) and the test-field model (TFM) presented here is an attempt to discover just how much the effects of scalar intermittency upset the applicability of two-point closures, and in what spectral regions. The present study is limited to $R_\lambda < 30$, with an even more severe limitation on P_λ (< 15). These limitations are dictated by machine limitations (within Cray IA memory). The numerical code consists of an extension of the Superbox code of Orszag & Patterson (1972*a*) to include

† Present address: NASA, Ames Research Center, M.S. 202A-1, Moffett Field, CA 94035, U.S.A.

a scalar field. It should be noted that experimentally the scalar intermittency does not disappear at low R_λ (Freymuth 1978) or the present DNS (Kerr 1981).

Section 2 presents a brief review of the closure equations (DIA–TFM), together with a sketch of the numerical methods for the DNS. Both of these topics have been covered in some detail elsewhere (see e.g. Newman & Herring 1979; Larcheveque *et al.* 1980, for DIA–TFM; Kerr 1981, for DNS). For this reason, our discussion is limited to only those points needed for later discussions.

We should note at this point that both DIA and TFM must be regarded logically as spectral (or two-point) models of turbulence rather than rational approximations to the statistical aspects of the flow and scalar fields. This statement holds despite the fact that both these procedures were originally proposed in the context of (renormalized) perturbation theories, with Gaussian noise somehow as the zeroth-order state. The convergence of such perturbation approaches at large Reynolds numbers is in serious doubt (see e.g. the discussion by Kraichnan 1971). Nonetheless they still embody many of the statistical aspects expected of real turbulence in a way which allows easy numerical (and especially analytic) computation. Included in the list of physically expected properties are the equipartitioning of variance among all available degrees of freedom, an eddy-viscous (or conductive) effect of small scales on large scales, and – for the TFM – a fidelity to the experimental inertial-range spectra. With regard to the last point, the DIA is known to yield a $k^{-\frac{3}{2}}$ inertial range instead of the proper $k^{-\frac{5}{3}}$ range. As we shall see, however, at low Reynolds numbers, it probably has more verisimilitude than TFM. This is because of its more realistic treatment (accompanied by the need for more numerical computation) of two-time or lagged-covariance aspects of the flow.

An important issue in connection with the use of statistical models of this sort is the question of computation time for DNS as compared to the statistical models, DIA or TFM. Even if the closures are accurate, their practical importance would be severely diminished if their numerical integration required more computer time than the DNS. Let us state at the onset of our discussion of the point the computer time t_c for the present calculations: DNS, $t_c = 100\,\mathrm{s}$; DIA, $t_c = 30\,\mathrm{s}$; TFM, $t_c = 0{\cdot}5\,\mathrm{s}$. All calculations were performed on the NCAR Cray I computer, and the corresponding programs vectorized insofar as permitted by FORTRAN. (The DNS contains a CAL FFT as an essential component.) For the DNS, five runs were required to secure good statistics. However, the above data is not a good guide for estimating the relative utility of these methods. The point is that the statistical theories may easily be extended to much higher Reynolds numbers by analytically using spectral smoothness with only a modest increase of their t_c values, while the DNS (32^3) cannot be extended beyond $R_\lambda \simeq 40$ without significant high-wavenumber truncation errors. On the other hand, the DIA t_c increases as $t_{\max}^3$, where $t_{\max}$ is the duration of integration. Thus a straightforward timestepping of the DIA quickly becomes prohibitive. Again, temporal smoothness of the two-time spectral functions may be used to increase the numerical efficiency.

Section 3 presents a comparison of theory and simulations, with some special focus on the behaviour of the small scales (dissipation range). In this region, we find a better agreement between DIA and DNS than TFM and DNS. The reason for this appears to be related to the relatively long coherence times of the small scales; a two-time closure appears needed to describe these effects. The TFM *genre* closure (single time)

appears inadequate regardless of the values of the adjustable parameters (g_v and g_θ).

Finally, §4 compares the present theoretical numerical results (DIA, TFM and DNS) with the low-R_λ experiments of Tavoularis *et al.* (1978). Here, DNS results for the course of $\langle(\partial u/\partial x)^3\rangle/\langle(\partial u/\partial x)^2\rangle^{\frac{3}{2}}$ as a function of R_λ as well as that for DIA appear to be in good agreement with experiment down to $R_\lambda \simeq 1$. This is not true for the TFM, for reasons noted above.

2. Equations of motion and theoretical concepts

We consider a homogeneous field of turbulence $\mathbf{u}(\mathbf{x}, t)$ together with a scalar $\theta(\mathbf{x}, t)$ satisfying

$$\partial_t \mathbf{u} = -\nabla p - (\mathbf{u}.\nabla)\mathbf{u} + \nu\nabla^2\mathbf{u}, \tag{1}$$

$$\partial_t \theta = -(\mathbf{u}.\nabla)\theta + K\nabla^2\theta, \tag{2}$$

$$\nabla.\mathbf{u} = 0. \tag{3}$$

Here, ν and K are the kinematic viscosity and thermal diffusivity. Let $(\mathbf{u}, \theta)$ have at $t = 0$ multivariate homogeneous Gaussian statistics, and further suppose that $\langle\mathbf{u}(\mathbf{x}, 0)\theta(\mathbf{x}', 0)\rangle = 0$ for all $(\mathbf{x}, \mathbf{x}')$. The problem considered here is then to determine the subsequent statistical moments, $\langle\mathbf{u}(\mathbf{x}, t)\mathbf{u}(\mathbf{x}', t')\rangle$, $\langle\mathbf{u}(\mathbf{x}, t)\theta(\mathbf{x}', t')\rangle$, $\langle\theta(\mathbf{x}, t)\theta(\mathbf{x}', t')\rangle$, ..., for all $(\mathbf{x}, t)$ and $(\mathbf{x}', t')$, $(t, t') > 0$. The DIA furnishes a partial (*approximation*) answer to this question by prescribing full second-moment equations of motion. Denoting

$$U(k, t, t') = \langle u_i(\mathbf{k}, t)\, u_i(-\mathbf{k}, t')\rangle,$$

$$\Theta(k, t, t') = \langle\theta(\mathbf{k}, t)\theta(-\mathbf{k}, t')\rangle,$$

where

$$(\mathbf{u}(\mathbf{x}), \theta(\mathbf{x})) = \sum_{\mathbf{k}} \exp(i\mathbf{k}.\mathbf{x})\,(\mathbf{u}(\mathbf{k}), \theta(\mathbf{k})).$$

The DIA yields (see for example Kraichnan 1959; Newman & Herring 1979)

$$\partial_t U(k, t, t') = \int_\Delta dp\, dq\, B^u(k, p, q) \int_0^{t'} ds\, G^u(k, t', s)\, U(p, t, s)\, U(q, t, s)$$

$$- \int_0^t ds\, \eta^u(k, t, s)\, U(k, s, t') - \nu k^2 U(k, t, t'), \tag{4}$$

$$\partial_t \Theta(k, t, t') = \int_\Delta dp\, dq\, B^\theta(k, p, q) \int_0^{t'} ds\, G^\theta(k, t', s)\, U(q, t, s)\, \Theta(p, t, s)$$

$$- \int_0^t ds\, \eta^\theta(k, t, s)\, \Theta(k, s, t') - Kk^2 \Theta(k, t, t'). \tag{5}$$

Here

$$(\eta^u(k, t, s),\ \eta^\theta(k, t, s)) = \int_\Delta dp\, dq\, B^{u,\theta}(k, p, q)\, G^{u,\theta}(p, t, s)\, U(q, t, s), \tag{6}$$

$$(\partial_t + (\nu, K)k^2)\, G^{u,\theta}(k, t, t') = -\int_{t'}^t ds\, \eta^{u,\theta}(k, t, s)\, G^{u,\theta}(k, s, t'). \tag{7}$$

The coefficients $B^{u,\theta}(k,p,q)$ are

$$\left.\begin{aligned} B^u(k,p,q) &= p^2q(xy+z^3)\pi, \\ B^\theta(k,p,q) &= kpq(1-y^2)\pi, \\ (x,y,z) &= ((p^2+q^2-k^2)/2pq,\ (k^2+q^2-p^2)/2kq,\ (k^2+p^2-q^2)/2kp). \end{aligned}\right\} \tag{8}$$

In recording these equations, we have assumed isotropy, and that the heat-flux spectrum is identically zero. In addition, the integral over $dp\,dq$ is over all (p,q) that can form a triangle.

For $\nu = K = 0$, these equations satisfy an important thermal-equilibrium constraint; the fluctuation dissipation theorem (Kraichnan 1958):

$$\left.\begin{aligned} U(k,t,t') &= G(k,t,t')\,U(k,t',t'), \\ U(k,t,t') &= \text{const.} \end{aligned}\right\} \tag{9}$$

The DIA is defective (Kraichnan 1965) in that it does not distinguish properly between large-scale convection and straining. This leads to a spurious $k^{-\frac{3}{2}}$ inertial range instead of the correct $k^{-\frac{5}{3}}$. However, at moderate R_λ (i.e. in a wind tunnel), comparisons with both numerical simulations and experimental data indicate that the consequences of this error are not significant (Herring & Kraichnan 1972). Subsequent to its original introduction, Kraichnan (1965, 1971) proposed methods of avoiding this dilemma, the most consistent of which is the Lagrangian-history direct-interaction approximation. This procedure deals with equations similar in complexity to (4) and (5), except that (t,t') are replaced by 'Lagrangian times', which in some sense track the motion of fluid parcels. This procedure, and particularly its later manifestations (see Kraichnan & Herring 1978; Herring & Kraichnan 1979), has proved to be a fairly accurate tool for describing the statistical dynamics of turbulent flows. It is, however, rather unwieldy; in fact, even the DIA is somewhat inconveniently complicated as a computational tool.

A computationally more convenient method is the TFM (Kraichnan 1971), which requires only one time argument; its basic dynamical ingredient is $U(k,t,t)$. This procedure properly yields $k^{-\frac{5}{3}}$ at large R_λ; and, in particular, recent comparisons with experiments at large R_λ show it to be fairly accurate for both U and Θ (Larcheveque *et al.* 1980). The TFM utilizes (9) (unjustifiably extended out of thermal equilibrium) to eliminate two-time arguments from consideration, and then prescribes a properly Galilean-invariant equation to replace (7). These replacements, although structurally similar to (7), differ in that the coefficients $B^u(k,p,q)$ and the time-history integrals are altered so as to yield a properly Galilean equation for $g(k,t,t')$ (i.e. one insensitive to large-scale translation). The time-historical modifications involve a 'Markovianization', which is necessary if purely Eulerian invariant description is to be retained. The resulting set of TFM equations for $U(k,t,t)$ and $\Theta(k,t,t)$ are

$$\begin{aligned} \partial_t U(k,t,t) = &\int_\Delta dp\,dq\,B^u(k,p,q)\,D^{111}(k,p,q)\,[U(p,t,t)-U(k,t,t)]\,U(q,t,t) \\ &-2\nu k^2\,U(k,t,t), \end{aligned} \tag{10}$$

$$\begin{aligned} \partial_t \Theta(k,t,t) = &\int_\Delta dp\,dq\,B^\theta(k,p,q)\,D^\theta(k,p,q)\,U(q,t,t)\,[\Theta(p,t,t)-\Theta(k,t,t)] \\ &-2\kappa k^2\,\Theta(k,t,t), \end{aligned} \tag{11}$$

where

$$D^u(k,p,q) = G^u(k,t,0)\,G^u(p,t,0)\,G^u(q,t,0),$$

$$D^\theta(k,p,q) = \int_0^t G^\theta(k,t,s)\,G^\theta(p,t,s)\,G^1(q,t,s)\,ds,$$

The G here satisfy

$$(\partial_t + \nu k^2)\,G^i(k,t,s) = -\overline{\eta}^i(k)\,G^i(k,t,s), \quad (\partial_t + Kk^2)\,G^\theta(k,t,s,) = -g_\theta{}^2\overline{\eta}^\theta(k)\,G^\theta(k,t,s),$$

$$\overline{\eta}^i(k) = 2^{i-1}\,g_v^2 \int dp\,dq\,C(k,p,q)\,D^{i,3-i,1}(k,p,q)\,U(q,t,t). \tag{12}$$

Note that (10)–(12) contain no historical integrals, since they have been eliminated by the 'Markovian' assumption. We refer to Newman & Herring (1979) and/or Larcheveque *et al.* (1980) for a more complete description. We note that, if the right-hand side of (12) is set to zero, we recover the Markovian quasinormal approximation, recently revived by Tatsumi, Kida & Mizushima (1978). The η here contain 'rescaling' factors g_v, g_θ that must be fixed through a comparison with either a more secure theory or experiment. The choice $(g_v, g_\theta) = (1{\cdot}17, 0{\cdot}50)$ appears in good agreement with large R_λ and P_λ data (see e.g. Larcheveque *et al.* 1980).

The TFM for $U(k)$ has been compared to numerical simulations of Orszag & Patterson (1972) (Herring & Kraichnan 1972) and both $U(k)$ and $\Theta(k)$ have been compared to planetary-boundary-layer data by Larcheveque *et al.* (1980). However, comparison of $\Theta(k)$ to DNS results for either DIA or TFM has not been reported. We view the last step as important in establishing the fidelity of any closure, particularly for the scalar problem, for which the importance of intermittency is experimentally indicated, and also in view of the rather ambiguous results obtained earlier for wind-tunnel experiments (Newman & Herring 1979).

The DNS is based on the Superbox code introduced by Orszag & Patterson (1972*a*, *b*), and subsequently modified for the Cray IA by Siggia (1981). In Superbox the velocity is de-aliased by truncating interactions outside a sphere and using two shifted grids to calculate transfer rates. Our code continues to truncate interactions outside a sphere, but uses only one grid. This means that the velocity field is treated pseudospectrally or aliased. On the other hand, the scalar field is de-aliased in the following manner: compute the scalar transfer in both the conservative and nonconservative form, and advance the scalar using the average of the two. The details of this method are discussed by Kerr (1981). All the computations are on a 32-cubed grid, with wavenumber range $1 \leqslant \frac{1}{2}k \leqslant 16$. This code operates in memory on the CRAY IA. The code is currently being modified to perform 64-cubed calculations out of memory.

3. Comparison of DNS, TFM and DIA

We consider first the following initial spectrum for $E_v(k) = 2\pi k^2 U(k,0)$ and $E_\theta(k) = 2\pi k^2\,\Theta(k)$ (run 1):

$$E_v(k) = A_v k^4 \exp(-B_v k^2), \tag{13}$$

$$E_\theta(k) = A_\theta k^4 \exp(-B_\theta k^2), \tag{14}$$

where

$$A_v = 6\pi^{\frac{1}{2}} B_v^{\frac{3}{2}}, \quad A_\theta = 12\pi^{\frac{1}{2}} B_\theta^{\frac{3}{2}}, \quad B_v = B_\theta = 0{\cdot}0220971.$$

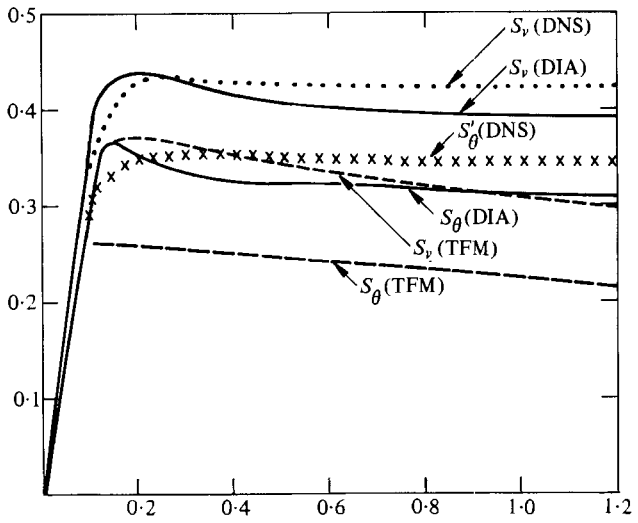

FIGURE 1. Comparison of velocity and mixed scalar skewness (see (15) and (16)) (S_v, S'_θ) for DNS, TFM, and DIA. Initial conditions are given by (13) and (14).

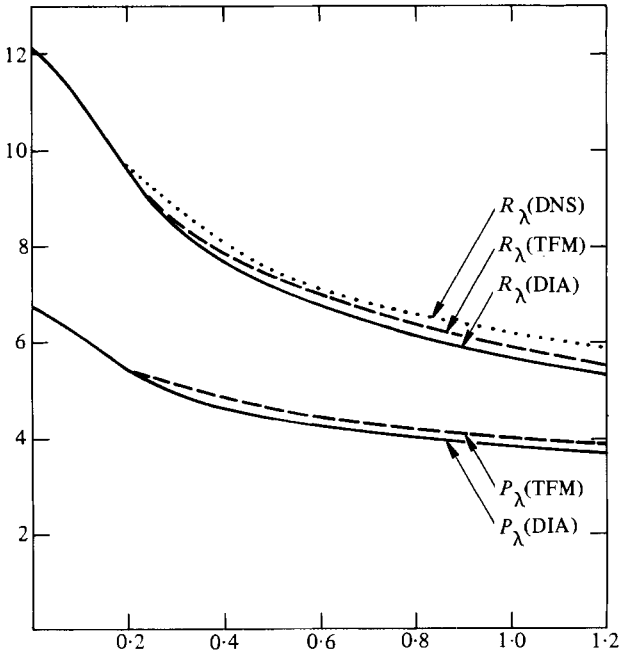

FIGURE 2. Course of R_λ and P_λ for run 1 ((13) and (14) give initial conditions for $E_v(k)$ and $E_\theta(k)$).

We should note here that our choice of initial data (13), (14) is made as a convenient set for a numerical comparison of theory and simulation. In particular (14) behaves differently as $k \to 0$ than that proposed by Corrsin (1951) on the basis of Loitsiansky-like considerations for the scalar field. Both (13) and (14) appear to preserve their $k \to 0$ form as the spectra evolve according to all three methods investigated and are

consistent with the proposal of Lesieur & Schertzer (1978). As noted earlier, the computational wavenumber domain is (2, 32). The values of ν and K are 0·01 and 0·02 respectively ($Pr = 0{\cdot}5$). With these values of ν, K, B_v and B_θ (see (13), (14)), $R_\lambda(t = 0) = 12{\cdot}0$, while $P_\lambda = 6{\cdot}0$. This rather small value for P_λ was found necessary in order to avoid significant truncation errors for $E_\theta(k)$ near $k = 32$. For the velocity field, the truncation errors are not as severe, indicating a larger transfer for the scalar field than for the velocity. Convenient non-dimensional measures of the magnitude of energy and scalar-variance transfer to large wavenumber are the derivative skewnesses. There are three experimentally measurable skewnesses, two of which are related to the transfer. The velocity skewness is

$$S_v = \langle(\partial u/\partial x)^3\rangle \langle(\partial u/\partial x)^2\rangle^{-\frac{3}{2}} = \frac{2}{35}\int k^2 T_u(k)\, dk\, (\dot{E}_v/15\nu)^{-\frac{3}{2}}. \tag{15}$$

For the scalar transfer the equivalent measure is the mixed skewness

$$S_\theta = \langle(\partial u/\partial x)(\partial\theta/\partial x)^2\rangle \langle(\partial u/\partial x)^2\rangle^{-\frac{1}{2}} \langle(\partial\theta/\partial x)^2\rangle^{-1}$$
$$= \frac{2}{15}\int k^2 T_\theta(k)\, dk\, (\dot{E}_v/15\nu)^{-\frac{1}{2}} (\dot{E}_\theta/6K)^{-1}. \tag{16}$$

The third measurable skewness, the scalar skewness $\langle(\partial\theta/\partial x)^3\rangle$, is zero in isotropic calculations such as ours. T_v and T_θ, the energy and variance transfer functions, are defined by $(\dot{E}_v, \dot{E}_\theta) = (T_v, T_\theta) - 2(\nu, K)k^2(E_v, E_\theta)$. Figure 1 compares the course of (S_v, S_θ) for $(0 < t < 1{\cdot}2)$. The rise of S from its initial zero Gaussian value to its saturated value ($S \simeq 0{\cdot}4$), after which self-similarity of the small scales sets in, is clearly seen. The values shown here do not differ much from those reported at much larger R_λ and P_λ, which suggests a rough R_λ independence of the dissipation ranges.

Figure 2 compares the course of $R_\lambda(t)$ and $P_\lambda(t)$ during the time span covered. A certain amount of the initial rapid decline of R_λ and P_λ is accounted for by the surge of energy and scalar variance to small scale during the build-up phase for S_v and S_θ. We note that, at $t = 1$, both R_λ and $P_\lambda \lesssim 10$, yet S_v and S_θ remain rather close to their large (R_λ, P_λ) saturated values.

Figures 3 (*a*, *b*) compare the course of energy spectra $E_v(k)$ and $E_\theta(k)$ for DIA and TFM to DNS. For a given initial spectrum it was necessary to make several DNS runs with different initial random kernels in order to get stable satistics. The DNS points here represent an ensemble of five runs. Ensembles of this size were found necessary in order to reduce the scatter of the DNS scalar $E_\theta(k)$ to an acceptable level (1 % error). At large k, the DIA appears to be the superior method. The TFM cannot be improved significantly by decreasing g_v, g_θ (as would be needed to increase E_v, E_θ). The values of R_λ, P_λ are so small that the TFM differs little from the Markovian quasinormal theory (for which $g_v = g_\theta = 0$) for the present run. We believe that TFM discrepancy is a result of Markovianization, which should decrease the energy transfer to large k. This may be seen by considering the DIA and its corresponding Markovianized version (the generalized Edward's theory discussed by Herring & Kraichnan (1972)). The computed value of S_v for the latter during free decay appears to be about 30 % smaller than the former.

The enhanced DIA energy transfer (relative to TFM) follows from its fidelity to the possible existence of near-laminar flow (long Eulerian correlation times) and to the

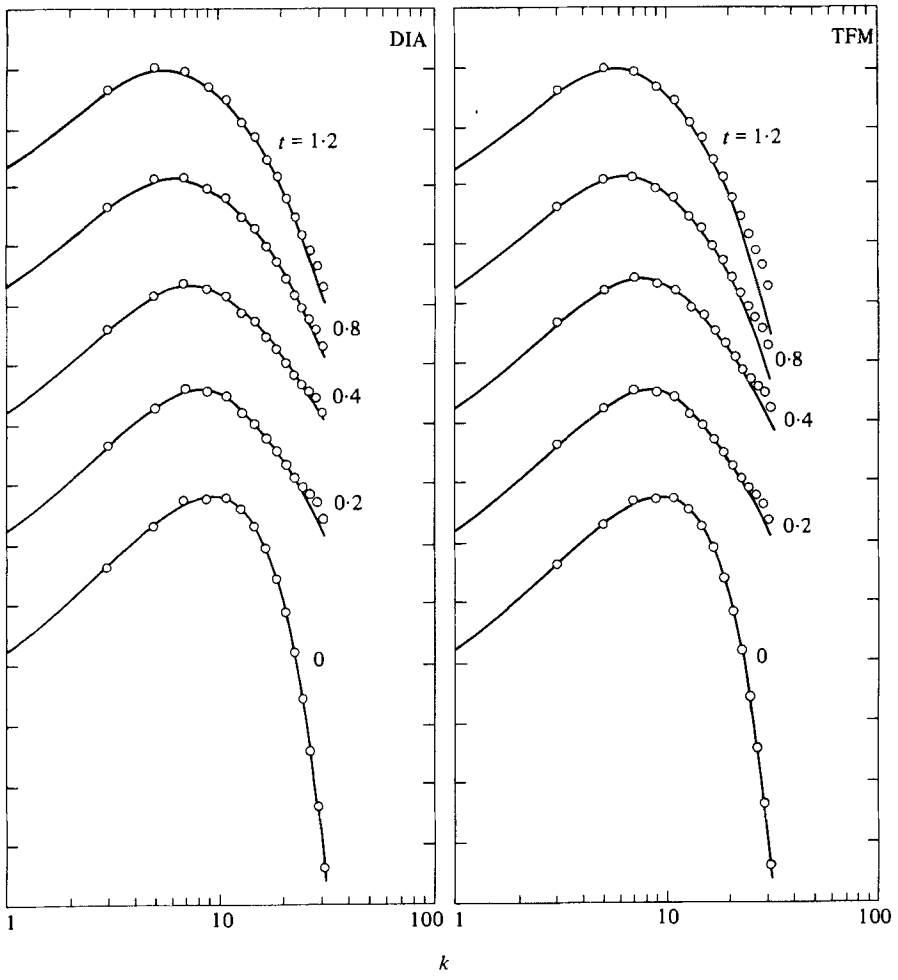

(a)

FIGURE 3 (a). For caption see opposite page.

fact that such flows have a more efficient transfer. This aspect of the DIA was first noted by Kraichnan (1964), and observed in the numerical DIA treatment of thermal large-Prandtl-number convection (Herring 1969). Later it was used by Herring (1977) in treating turbulence interacting with a random topography. It may be demonstrated directly from (4)–(7) that these equations are consistent with a static $U(k,t,t')$ (i.e. an independence with respect to $t-t'$), provided a consistent forcing function is added to make (4), (5) stationary. It is of interest in this connection to examine the DIA's two-time structure to see in what respect the lagged autocovariance exceeds the expectation of the fluctuation dissipation theorem (9). To do this we compare

$$R^*(k,t,t') = U(k,t,t')/U(k,t',t') \tag{17a}$$

and

$$\tilde{R}^*(k,t,t') = \Theta(k,t,t')/\Theta(k,t',t') \tag{17b}$$

to $G^u(k,t,t')$ and $G^\theta(k,t,t')$ for $k = 4{\cdot}9$ and $k = 20{\cdot}3$ in figures 4 (a, b). The comparison

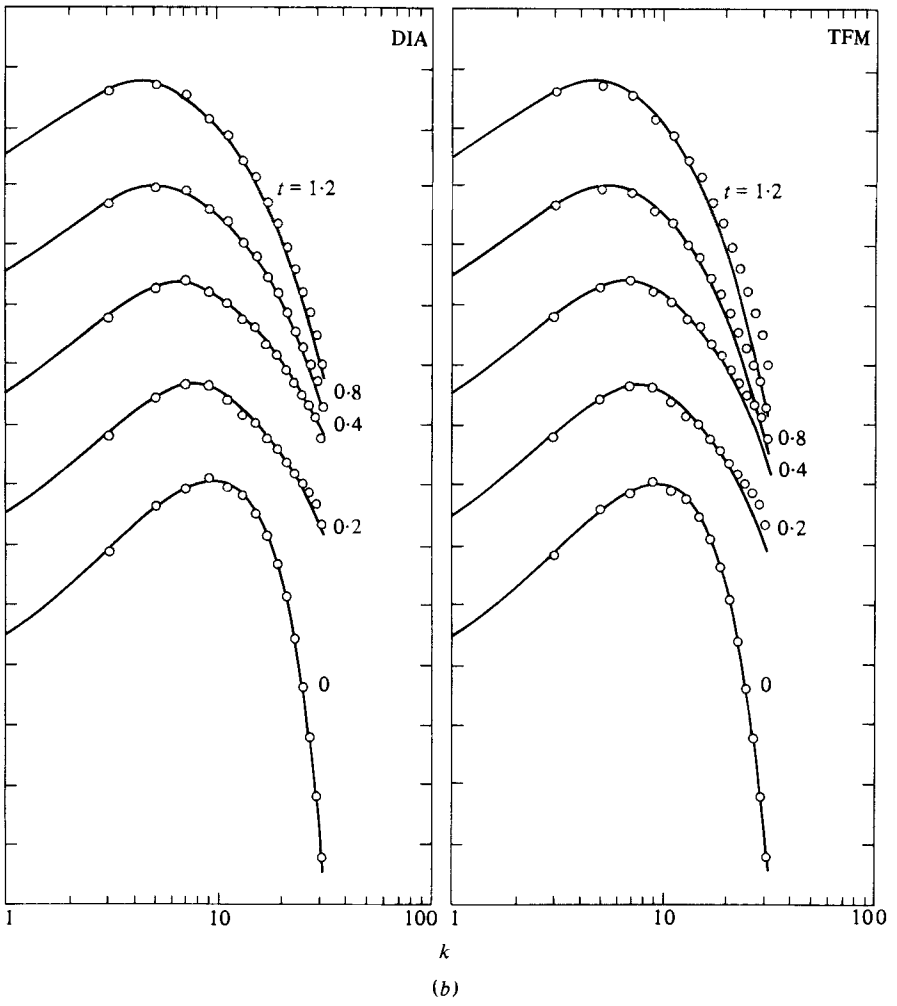

FIGURE 3. Comparison of energy spectra $E_v(k)$, $E_\theta(k)$ during the course of run 1. (*a*) compares DNS to DIA and TFM for E_v; (*b*) compares DNS to DIA and TFM for $E_\theta(k)$. comparisons are made for t = 0, 0·2, 0·4, 0·8 and 1·2. Initial E_v and E_θ are (13) and (14), Pr = 0·5. Ordinate scale is logarithmic but arbitrary, with each succeeding spectrum displaced upward by two orders of magnitude.

is presented for $t' = 2$, so that the abscissa is $2-t$. The two values of k were chosen to be near the energy peak and in the far-dissipation range, where nonlinearities are in equilibrium with molecular dissipation. To relate these values of k to the dynamics of energy transfer, we refer to figure 4(*c*), which gives $T_{v,\theta}(k)$ for $t = 2$. We note from figures 4(*a*, *b*) that $R^* \simeq G^u$ ($\tilde{R}^* \simeq G^\theta$) in the energy-containing range, while R^* ($\tilde{R}^*$) substantially exceeds G^u (G^θ) in the far-dissipation range. This last region is precisely where the TFM most significantly underestimates $T_{v,\theta}(k)$ through its use of (9) to eliminate two-time Us from consideration.

Figures 5(*a*)–7(*b*) (for run 2) are identical to figures 1(*a*)–3(*b*) (run 1), with the sole difference that A_v and A_θ are increased to

$$A_v = 30\tfrac{1}{2}B_v^{\frac{3}{2}}, \qquad A_\theta = 60\tfrac{1}{2}B_v^{\frac{3}{2}}. \qquad (18), (19)$$

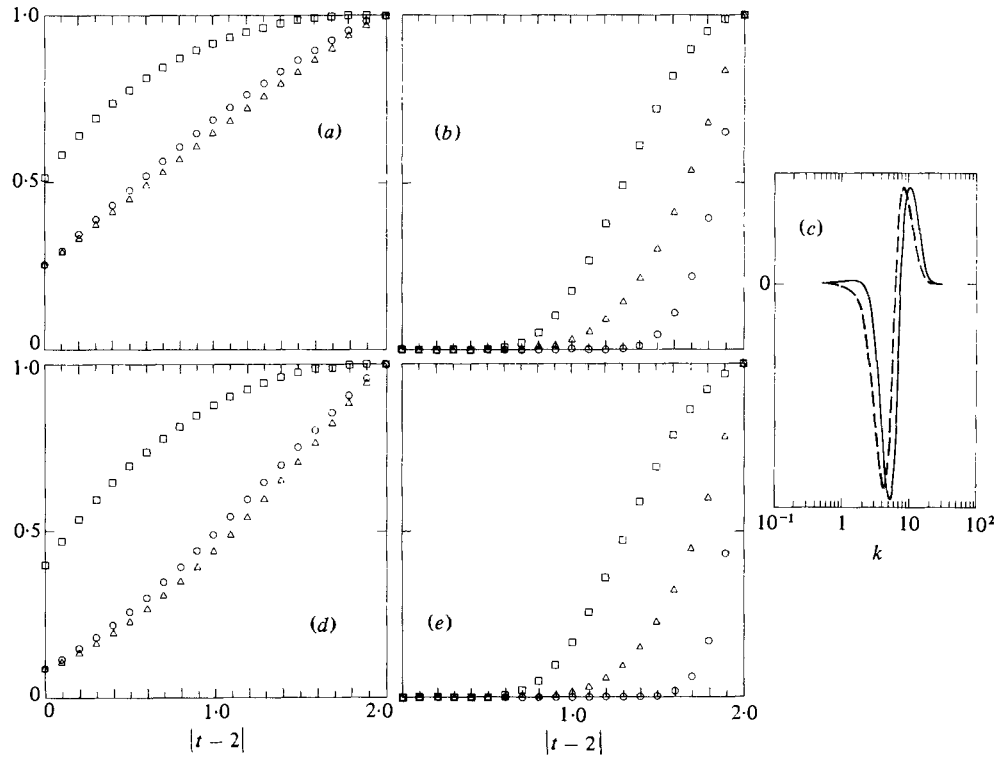

FIGURE 4. Comparison of DIA $G(k, t, t')$ (○), $U(k, t, t')/U(k, t', t')$ (△) and $U(k, t, t')$ $[U(k, t, t) \times U(k, t', t')]^{\frac{1}{2}}$ (□) at $t' = 2$ for $k = 4{\cdot}5$ (*a*), and $k = 22{\cdot}5$ (*b*). (*c*) shows $T_v(k, 2)$ (——) and $T_\theta(k, 2)$ (– – –) (ordinate units arbitrary). (*d*) and (*e*) similarly depict $G^\theta(k, t, t')$, $\Theta(k, t, t')/\Theta(k, t', t')$, and $\Theta(k, t, t')$ $[\Theta(k, t, t)\ \Theta(k, t', t')]^{\frac{1}{2}}$.

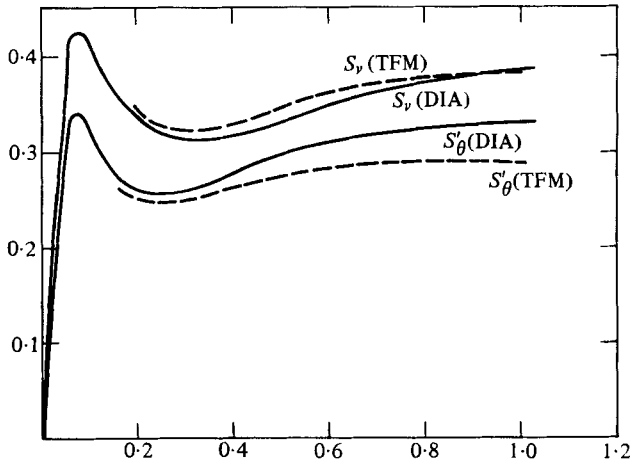

FIGURE 5. S_v and S_θ comparisons for run 2 ((13) and (14) for $E_v(k)$, $E_\theta(k)$, with A_v and A_θ given by (18) and (19)).

Run 2 is thus at somewhat higher R_λ and P_λ. We note that, in this case, the TFM results are in better agreement at large k. However, the calculation does not reach as far into the dissipation range as does run 1. There also appears to be evidence of large-k truncation effects in all methods, as is especially evident in figure 5 (*a*).

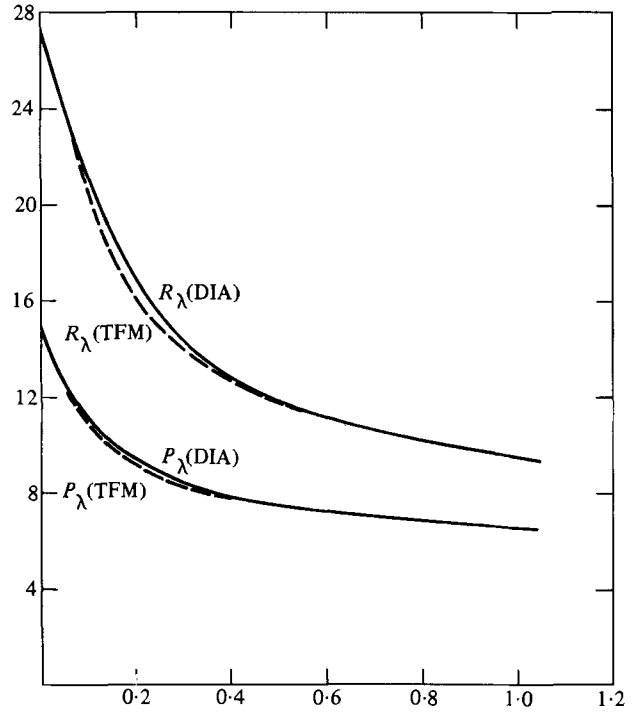

FIGURE 6. R_λ and P_λ comparisons for run 2. ((13) and (14) give initial conditions for $E_v(k)$ and $E_\theta(k)$.)

4. Comparison of present results to low-Reynolds-number data for S_v

Tavoularis, Bennett & Corrsin (1978) have reported wind-tunnel measurements of $S_v(R)$ down to $R_\lambda = 1$. We compare our results for S_v to their assembled measurements in figure 8. We note that DIA tends to overestimate S_v, as $R_\lambda \to 0$, while TFM underestimates it. This is in rough agreement with our observations of §3. Both theoretical calculations have some hystereses; S_v depends to a certain extent (about 5 %) on not only the current R_λ, but also on the value of $R_\lambda(t = 0)$. There may be residuals of the initial Gaussian state which longer run times may eliminate. At larger R_λ (> 20), TFM is in reasonable agreement with experiment; we do not, however, see in the TFM theoretical results the apparent dip in the data near $R_\lambda = 100$. The DIA begins to underestimate S_v significantly for $R_\lambda \gtrsim 50$, beyond which the Galilean non-invariance – the most significant qualitative error of this theory – begins to cause detectable errors in the spectrum. We do not know of equivalent observational summaries of the Θ-data.

Our DNS results for $S_v(R_\lambda)$ should also be compared to the recent numerical simulations of Schirani & Ferziger (1982), who report an $S_v(R_\lambda)$ curve having a maximum at $R_\lambda \simeq 10$. This is contrary to our results, which indicate a monotonically increasing S_v *vs.* R_λ curve. Their results were obtained with a 16^3 grid. For $R_\lambda > 20$ they used an eddy viscosity. There is no reason that with an eddy viscosity these small scales would give the correct skewness. Siggia (1981) has produced results consistent with ours with a 64^3 grid and $R_\lambda = 45$.

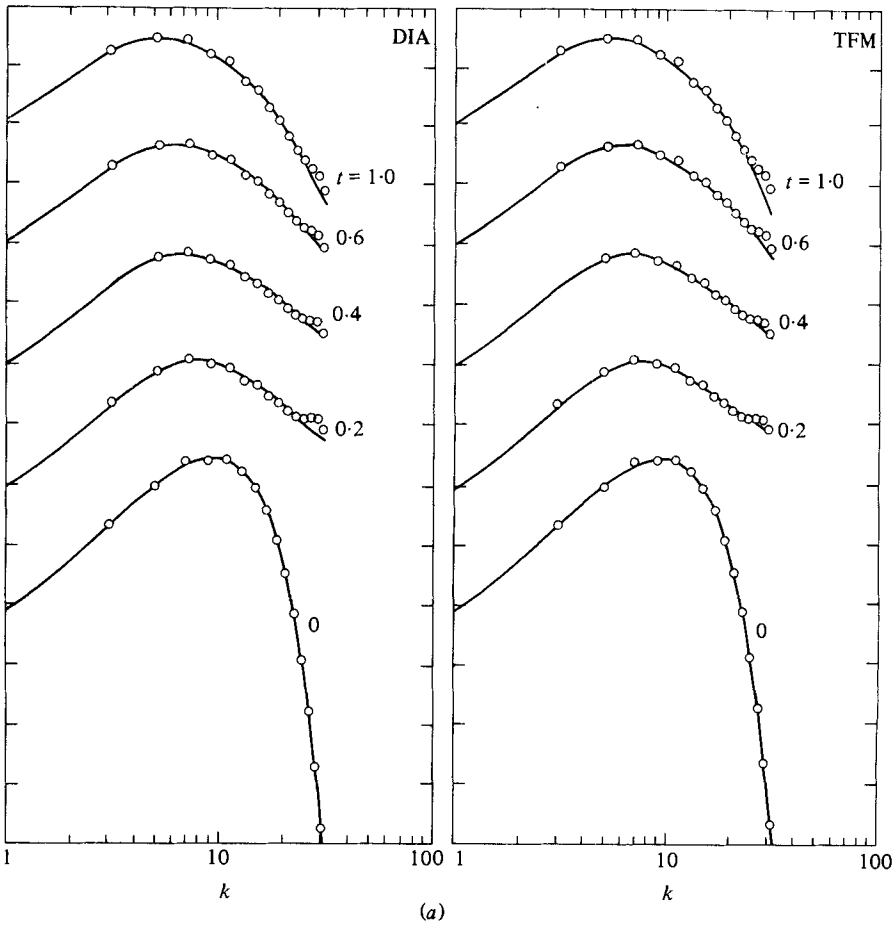

FIGURE 7(a). For caption see opposite page.

The TFM results presented here for large R_λ have been gleaned from other calculations (Herring & Kraichnan 1972; Larcheveque *et al.* 1980; Herring *et al.* 1981). We note that S_v has not reached its $R_\lambda \to \infty$ asymptote even at $R_\lambda = 1000$. This would appear to be frustrating to efforts to ascribe to the increase of S_v with R_λ a strong non-Gaussianity, as has been done, for example, by Van Atta (1974).

It should be noted that our theoretical calculations (DNS, DIA and TFM) are for $E_v(k) \simeq k^4$ as $k \to 0$, which is not necessarily the experimental shape (Tavoularis *et al.* (1978), in fact, make a strong case for k^2). However, previous numerical experience using DIA–TFM calculations suggests that $S_v(R_\lambda)$ is not strongly dependent on this spectral region.

5. Concluding comments

The comparison of DIA and TFM closures to the DNS presented here indicates that both procedures are in good agreement in the energy-containing range. Our comments apply only to R_λ and $P_\lambda \lesssim 30$, a limitation imposed by machine considerations in

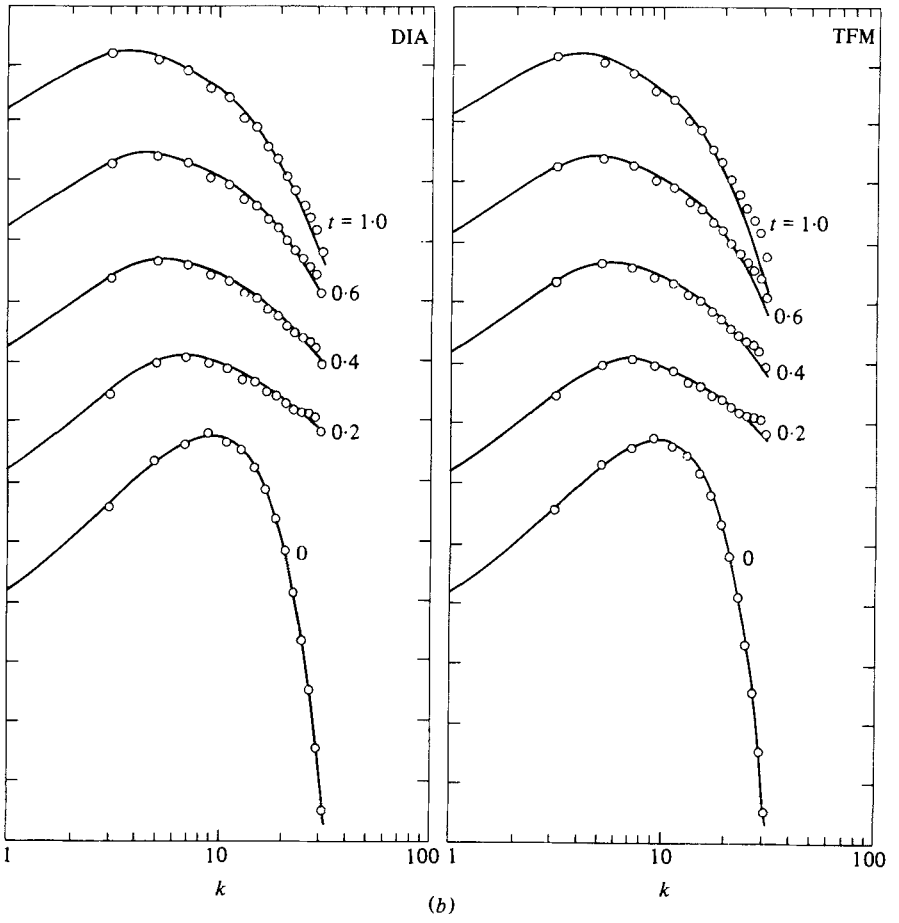

FIGURE 7. Comparison of $E_v(k)$ and $E_\theta(k)$ for run 2.
See caption to figure 3 for further details.

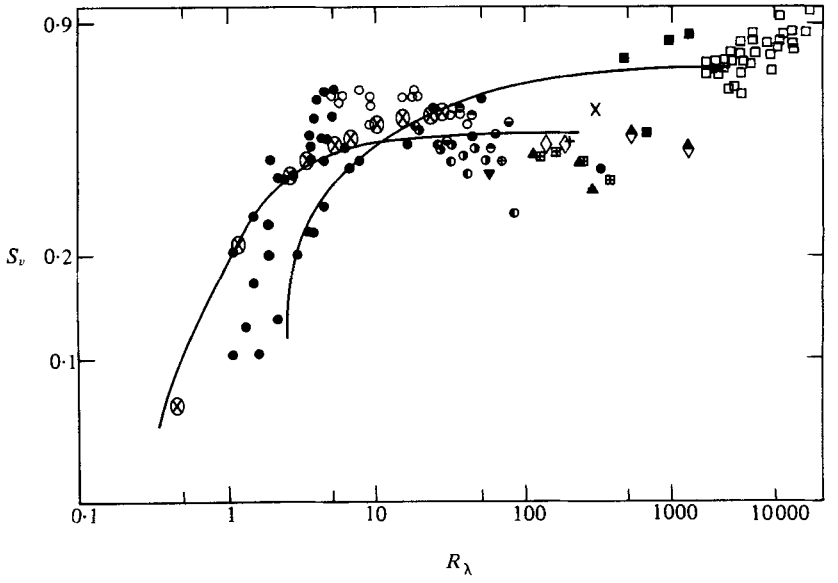

FIGURE 8. Comparison of low-R_λ $S_\theta(R_\lambda)$ data of Tavoularis *et al.* (1978) with DNS (⊗), TFM, DIA (solid lines, with TFM > DIA at large R_λ).

treating the DNS. At quite small R_λ, or perhaps equivalently in the far-dissipation range, the TFM does have significant errors (as may be noted from figure 3) attributable to its use of a Markovianization, in connection with the use of the fluctuation dissipation equation (9). Otherwise, the agreement with DNS is encouraging in view of the shaky comparisons made earlier to the experimental data, as reported, for example, by Newman & Herring (1979). It suggests that the data may be affected by anisotropy even at small scales, a condition which the DNS avoids. At larger R_λ the TFM's overall accuracy seems to improve, suggesting that its Markovianization errors are buried deeper in the dissipation range, where they go unnoticed.

It is somewhat surprising that our calculations have uncovered a significant discrepancy in the TFM at such small R_λ and P_λ. Naively, one would have thought that all reasonable perturbation procedures would converge as $(R_\lambda, P_\lambda) \to 0$. Of course, what we see here as $R_\lambda \to 0$ is a qualitative failure of the TFM: the assumption that the flow is turbulently active (in the sense of (9)) becomes untenable and must be replaced by an assumption of near-laminar flow – especially at small scales. As noted in §3, no sensible adjustment of the scaling parameters g_v, g_θ can restore agreement (for run 1) at large k since calculations with $(g_v, g_\theta) = (0, 0)$ virtually superimpose those with $(g_v, g_\theta^2) = (1{\cdot}17, 0{\cdot}5)$. We have cited the fact that the DIA – in contrast to TFM – allows for long coherence times, and we have implied that the improved DIA agreement with DNS is attributable to this fact. We have not checked here that the DNS does in fact have long coherence times at small scales. Such a comparison has been reported at larger R_λ (for the velocity field only) by Orszag & Patterson (1972*b*), where it was noted that the DIA gave satisfactory results at moderate k, with increasing errors as k increases. In any case, the DIA gave the correct qualitative trend. It would be of value to have such results at lower R_λ and P_λ, where DIA should be more accurate at all k.

We have not discussed here the importance of intermittence and non-strong non-Gaussianity, especially in the scalar field. This is described in detail elsewhere (Kerr 1981). Here we only note that such effects are present, even at these modest values of R_λ and P_λ in the DNS. For example, the scalar derivative flatness factor for run 1 is approx. 3·8, as compared to the Gaussian value of 3. The importance of such effects appears, however, not to preclude agreement of second-order moments closure results with the reality of DNS.

R.M.K. acknowledges support from NSF Grant ENG-7902942. The National Center for Atmospheric research is sponsored by the National Science Foundation.

REFERENCES

Corrsin, S. 1951 The decay of isotropic temperature fluctuations in an isotropic turbulence. *J. Atmos. Sci.* **18**, 417–423.

Freymuth, P. 1978 Characterization of turbulent temperature ramps by two length scales. *Phys. Fluids* **21**, 2114.

Frisch, U. & Morff, R. H. 1981 Intermittency in non-linear dynamics and singularities for complex times. *Phys. Rev.* A **23**, 2673–2705.

Herring, J. R. 1969 The statistical theory of thermal convection at large Prandtl number. *Phys. Fluids* **12**, 2106–2110.

Herring, J. R. 1977 On the statistical theory of two-dimensional topographic turbulence. *J. Atmos. Sci.* **34**, 1731–1750.

HERRING, J. R. & KRAICHNAN, R. H. 1972 Comparison of some approximations for isotropic turbulence. In *Statistical Models and Turbulence* (ed. M. Rosenblatt & C. Van Atta), Lecture Notes in Physics, vol. 12, pp. 148–194. Springer.

HERRING, J. R. & KRAICHNAN, R. H. 1979 A numerical comparison of velocity-based and strain-based Lagrangian-history turbulence approximations. *J. Fluid Mech.* **91**, 581–597.

HERRING, J. R., SCHERTZER, D., LESIEUR, M., NEWMAN, G. R., CHOLLET, J. P. & LARCHEVEQUE, M. 1981 A comparative assessment of spectral closures as applied to passive scalar diffusion. Preprint; Submited to *J. Fluid Mech.*

KERR, R. M. 1981 Theoretical investigation of a passive scalar such as temperature in isotropic turbulence. Ph.D. thesis; Cooperative Thesis no. 64, Cornell University and National Center for Atmospheric Research.

KRAICHNAN, R. H. 1958 Irreversible statistical mechanics of incompressible hydrodynamic turbulence. *Phys. Rev.* **109**, 1407–1422.

KRAICHNAN, R. H. 1959 The structure of isotropic turbulence at very high Reynolds numbers. *J. Fluid Mech.* **5**, 497–543.

KRAICHNAN, R. H. 1964 Approximations for steady-state isotropic turbulence. *Phys. Fluids* **7**, 1163–1168.

KRAICHNAN, R. H. 1965 Lagrangian-history closure approximation for turbulence. *Phys. Fluids* **8**, 575–598; erratum **9**, 1884.

KRAICHNAN, R. H. 1968 Small scale structure convected by turbulence. *Phys. Fluids* **11**, 945–953.

KRAICHNAN, R. H. 1971 An almost-Markovian Galilean-invariant turbulence model. *J. Fluid Mech.* **47**, 513–524.

KRAICHNAN, R. H. & HERRING, J. R. 1978 A strain-based Lagrangian-history turbulence theory. *J. Fluid Mech.* **88**, 355–367.

LARCHEVEQUE, M., CHOLLET, J. P., HERRING, J. R., LESIEUR, M., NEWMAN, G. R. & SCHERTZER, D. 1980 Two-point closure applied to a passive scalar in decaying isotropic turbulence. In *Turbulent Shear Flows* 2 (ed J. S. Bradbury, F. Durst, B. E. Launder, F. W. Schmidt & J. H. Whitelaw), pp. 50–66. Springer.

LESIEUR, M. & SCHERTZER, D. 1978 Dynamique des gros tourbillons et décroissance de l'énergie cinétique en turbulence tridimensionelle isotrope à grand nombre de Reynolds. *J. Méc.* **17**, 607–646.

NEWMAN, G. R. & HERRING, J. R. 1979 A test field model study of a passive scalar in isotropic turbulence. *J. Fluid Mech.* **94**, 163–194.

ORSZAG, S. A. 1974 Statistical theory of turbulence. In *Fluid Dynamics*: 1973 *Les Houches Summer School on Physics* (ed. R. Balian & J. L. Penbe), pp. 235–374. Gordon & Breach.

ORSZAG, S. A. & PATTERSON, G. S. 1972*a* Numerical simulation of turbulence. In *Statistical Models and Turbulence* (ed. R. Rosenblatt & C. Van Atta), Lecture Notes in Physics, vol. 12, pp. 127–147. Springer.

ORSZAG, S. A. & PATTERSON, G. S. 1972*b* Numerical simulation of three-dimensional homogeneous isotropic turbulence. *Phys. Rev. Lett.* **28**, 76–79.

SCHIRANI, E. & FERZIGER, J. H. 1982 Simulation of low-Reynolds-number isotropic turbulence including a passive scalar. Submitted to *J. Fluid Mech.*

SIGGIA, E. D. 1981 Numerical study of small-scale intermittency in three-dimensional turbulence. *J. Fluid Mech.* **107**, 375–406.

TATSUMI, T., KIDA, S. & MIZUSHIMA, J. 1978 The multiple-scale cumulant expansion for isotropic turbulence. *J. Fluid Mech.* **85**, 97–142.

TAVOULARIS, S., BENNETT, J. C. & CORRSIN, S. 1978 Velocity-derivative skewness in nearly isotropic turbulence. *J. Fluid Mech.* **88**, 63–69.

VAN ATTA, C. W. 1974 Influence of fluctuations in dissipation rates on some statistical properties of turbulence scalar fields $I_z v_0$. *Atmos. Ocean. Phys.* **10**, 712–719.

YEH, T. T. & VAN ATTA, C. W. 1973 Spectral transfer of scalar and velocity fields in heated-grid turbulence. *J. Fluid Mech.* **58**, 233–266.